

# Activation of Ultrathin Oxide Films for Chemical Reaction by Interface Defects

Jaehoon Jung,<sup>†,‡</sup> Hyung-Joon Shin,<sup>‡,§</sup> Yousoo Kim,<sup>\*,‡</sup> and Maki Kawai<sup>\*,†</sup>

<sup>†</sup>Department of Advanced Materials Science, The University of Tokyo, 5-1-5 Kashiwanoha, Kashiwa, Chiba 277-8561, Japan

<sup>‡</sup>RIKEN Advanced Science Institute, 2-1 Hirosawa, Wako, Saitama 351-0198, Japan

**S** Supporting Information

**ABSTRACT:** Periodic density functional theory calculations revealed strong enhancement of chemical reactivity by defects located at the oxide–metal interface for water dissociation on ultrathin MgO films deposited on Ag(100) substrate. Accumulation of charge density at the oxide–metal interface due to irregular interface defects influences the chemical reactivity of MgO films by changing the charge distribution at the oxide surface. Our results reveal the importance of buried interface defects in controlling chemical reactions on an ultrathin oxide film supported by a metal substrate.

Ultrathin oxide films grown on metal substrates are of great interest not only as supporting materials for chemically active nanoparticles but also as catalysts in the field of heterogeneous catalysis.<sup>1</sup> It has been recognized that the chemical reactivity of an ultrathin oxide film is closely related to the charging of adsorbate<sup>2–7</sup> from the oxide–metal interface and the changing of adhesion strength with strong polaronic distortion<sup>8,9</sup> between an oxide film and a metal substrate during chemical reaction. In addition, film thickness as a controllable dimension provides an opportunity to control the influence of the metal substrate support on the structure, charge, and adsorption energy of adsorbates on an oxide surface.<sup>3,5,8–14</sup> Therefore, ultrathin oxide films, such as MgO(100),<sup>4–9,13–15</sup> NiO(100),<sup>16</sup> Al<sub>2</sub>O<sub>3</sub>-(0001),<sup>3,17</sup> and FeO(111),<sup>18</sup> supported by metal substrates have been extensively studied as potential candidates for heterogeneous catalysts. Recently, using scanning tunneling microscopy and density functional theory (DFT), we demonstrated that the chemical reactivity for water dissociation on an ultrathin MgO film supported by Ag(100) substrate depends greatly on the film thickness.<sup>8,13</sup> Strengthening the interaction between the oxide and metal interface layers led to remarkably enhanced chemical reactivity of the ultrathin MgO film for water dissociation as compared to that achieved with its bulk counterpart.<sup>14,15</sup> Therefore, artificial manipulation of the local structure at the oxide–metal interface is expected to play a pivotal role in controlling the catalytic activity of oxide films. However, when compared to surface defects such as an O vacancy exposed on an MgO surface, few experiments concerning the oxide–metal interface—especially involving interface defects—have been performed due to the practical difficulties related to buried systems.<sup>19</sup> To fundamentally understand the structure–reactivity relationship at the oxide–metal interface, it is important to systematically

study how the chemical reaction depends on various types of irregular interface defects.

In this Communication, we report that structural imperfections at the oxide–metal interface clearly improve the chemical reactivity of a MgO film supported by an Ag substrate using spin-polarized periodic DFT calculations.<sup>20</sup> Water dissociation on three model systems with defects located at the oxide–metal interface of two-monolayer (2-ML) MgO/Ag(100)—an O vacancy (*int*-O<sub>vac</sub>), an Mg impurity (*int*-Mg<sub>imp</sub>), or an O impurity (*int*-O<sub>imp</sub>)<sup>21</sup>—has been examined and compared with the case of a MgO film with no defects (ND) (Figure 1).

The calculated formation energy of *int*-O<sub>vac</sub> (5.30 eV) is lower than that of surface O vacancy (*surf*-O<sub>vac</sub>, 6.16 eV), i.e., F<sup>0</sup> center, in agreement with previous computational data.<sup>12,22,23</sup> The existence of *int*-O<sub>vac</sub> was also suggested as the origin of tunneling barrier reduction in the metal/oxide/metal magnetic tunneling junction system.<sup>24</sup> Meanwhile, it can be expected that Mg or O impurity would also form in the Ag interface layer during rigorous MgO film growth. It is noteworthy that the calculated formation energies of *int*-Mg<sub>imp</sub> (0.45 eV) and *int*-O<sub>imp</sub> (1.49 eV) are much lower than that of *int*-O<sub>vac</sub>. Thus, the oxide film can play a role not only in providing a catalytic reactive site but also in stabilizing interface defects.

Figure 2 is a reaction energy diagram for water dissociation on the MgO/Ag(100) surface with and without interface defects. A water molecule first adsorbs asymmetrically on top of the surface magnesium atom, where one hydrogen atom interacts with a neighboring surface oxygen atom via hydrogen bonding. When the water molecule dissociates into H<sup>+</sup> + OH<sup>-</sup>, H<sup>+</sup> forms a hydroxyl ion (O<sub>s</sub>H) by bonding with a surface oxygen atom and OH<sup>-</sup> (O<sub>w</sub>H) bonds with the two nearest-neighboring magnesium atoms (“w” and “s” denote water and surface, respectively).<sup>7–9,13,25</sup> The energy diagram shows that the water molecule is more strongly adsorbed and more easily dissociated on the interface-defective MgO films compared to the ND MgO film (see Table S1 for the numerical values). Interestingly, the transition states (T) for the *int*-O<sub>vac</sub> and *int*-Mg<sub>imp</sub> locate below 0.0 eV, with transition state energies, *E*(T), of −0.18 and −0.01 eV, respectively. These cause the barrier heights (*E*<sub>a</sub>), *E*(T) − *E*(A), to be lowered and, accordingly, to be noticeably reduced by 42 (59)% and 29 (50)% from that of ND MgO film (*bulk* MgO). Along with the exothermic dissociation energy, *E*(D), for *int*-O<sub>vac</sub> (−0.26 eV) and *int*-Mg<sub>imp</sub> (−0.16 eV), the very low *E*(T) implies that water dissociation on the ultrathin MgO film surface

Received: January 27, 2011

Published: April 04, 2011

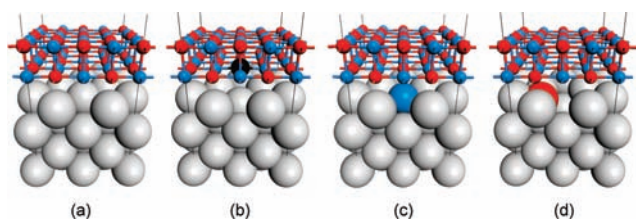


**Figure 1.** Optimized structures for an ultrathin MgO film deposited on an Ag(100) substrate with and without interface defects: (a) no defect (ND), (b) interface O vacancy (*int-O<sub>vac</sub>*), (c) interface Mg impurity (*int-Mg<sub>imp</sub>*), and (d) interface O impurity (*int-O<sub>imp</sub>*). Ag, gray; Mg, blue; O, red; O vacancy, black.

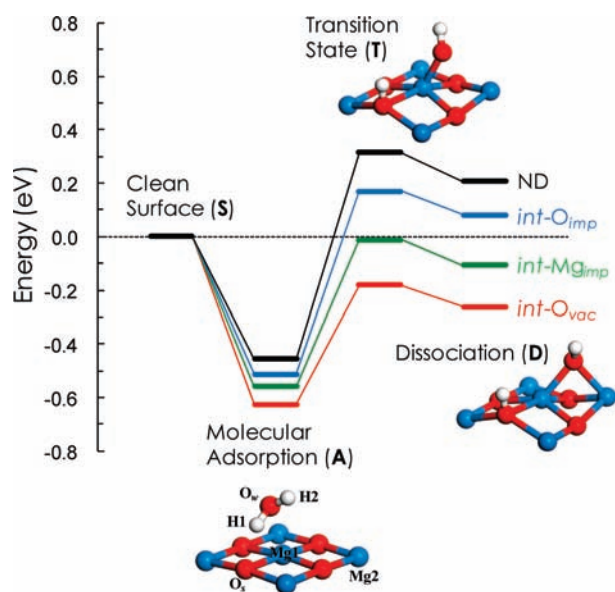


**Figure 2.** Reaction energy diagram (in eV) for the dissociation of a single water molecule on the non-defective (ND) and defective MgO/Ag(100) surfaces (*int-O<sub>vac</sub>*, *int-Mg<sub>imp</sub>*, and *int-O<sub>imp</sub>*). Non-dissociative adsorption (A), transition state (T), and dissociative adsorption (D) energies are evaluated relative to  $E(\text{H}_2\text{O}) + E(\text{substrate}) = 0$  eV. Mg, blue; O, red; H, white.

**Table 1. Net Charges (in  $e$ ) of the Ag Layer during Water Dissociation**

	ND	<i>int-O<sub>vac</sub></i>	<i>int-Mg<sub>imp</sub></i> <sup>a</sup>	<i>int-O<sub>imp</sub></i> <sup>a</sup>
S	-0.40	-1.54	-1.67 (+1.49)	+0.71 (-1.09)
A	-0.35	-1.60	-1.62 (+1.50)	+0.74 (-1.13)
D	-0.42	-1.57	-1.68 (+1.52)	+0.74 (-1.13)

<sup>a</sup>The atomic charge of the impurity atom doped in the Ag layer is given in parentheses.

with *int-O<sub>vac</sub>* or *int-Mg<sub>imp</sub>* does not require external thermal energy at the level of an individual molecule. Hence, even a small number of interface defects can supply plenty of opportunities to enhance chemical reactivity for water dissociation on an ultrathin MgO film surface.

The improved chemical reactivity of MgO films with interface defects can be explained by charge redistribution due to defect formation at the oxide–metal interface. MgO film growth on Ag substrate causes charge transfer at the interface from the MgO

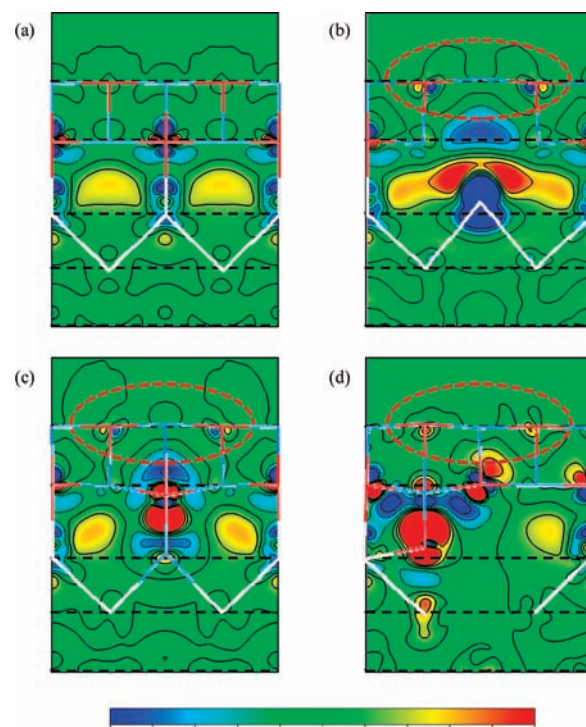


**Figure 3.** Charge density difference maps for non-defective and defective MgO/Ag(100) models: (a) ND, (b) *int-O<sub>vac</sub>*, (c) *int-Mg<sub>imp</sub>*, and (d) *int-O<sub>imp</sub>*. The atomic layers are indicated by black dashed lines. The scale is  $\pm 0.003 e/\text{bohr}^3$ . The cross-sectional structure is presented by colored solid lines: Ag, gray; Mg, blue; O, red.

layer to the Ag substrate.<sup>26</sup> Table 1 shows the net charge values of the Ag layer determined by Bader population analysis<sup>27,28</sup> during water dissociation on the MgO/Ag(100) surface with and without interface defects. The amount of charge transfer between MgO and Ag layers is increased by the formation of interface defects. Figure 3 shows the charge density difference maps of MgO/Ag(100) with and without interface defects. For MgO/Ag(100) with defects, the transferred charges are more highly localized at the oxide–metal interface than in the case of ND MgO/Ag(100). The distribution of localized electron density at the interface represents the electronic characteristics of each type of interface defect. The covalent-like interaction between the electrons trapped in *int-O<sub>vac</sub>* and the Ag substrate gives rise to a broader charge distribution (Figure 3b) than other types of defects (Figure 3c,d), which show ionic interactions between the MgO layer and impurity atoms embedded in the Ag substrate. These electronic characteristics are also confirmed by electron localization function (ELF) maps (see Figure S1). Our study reveals that charge localization at the interface strongly redistributes the local charge of the MgO surface (represented by dashed red circles in Figure 3). Therefore, the adsorption strength of water molecules and the further chemical reactivity of MgO films for water dissociation should be changed as a consequence of the strong charge localization at the oxide–metal interface, as shown in Figure 2. In particular, it is interesting to compare the MgO film with *int-O<sub>vac</sub>* with the gold cluster adsorbed on the *surf-O<sub>vac</sub>* of the MgO(100) surface. The catalytic activity of the gold cluster for CO oxidation can be activated by charge transfer from the *surf-O<sub>vac</sub>*.<sup>29</sup> Our result implies that the chemical reactivity of an oxide film can also be improved by charge transfer between the oxide film and a metal substrate.

**Table 2. Non-dissociative Adsorption Energy (in eV),  $E(A)$ , Net Charge (in  $e$ ) of Adsorbates,  $Q(\text{ads})$ , and Change of Bader Populations in the MgO Film ( $\Delta Q(\text{MgO})$ ) and Ag Substrate ( $\Delta Q(\text{Ag})$ ) during  $\text{O}_2$  and  $\text{H}_2\text{O}$  Adsorption on Non-defective (ND) and Defective ( $\text{int-O}_{\text{vac}}$ ) MgO/Ag(100) Surfaces<sup>a</sup>**

	$\text{O}_2$		$\text{H}_2\text{O}$	
	ND	$\text{int-O}_{\text{vac}}$	ND	$\text{int-O}_{\text{vac}}$
$E(A)$	-1.17	-1.67	-0.46	-0.62
$Q(\text{ads})$	-0.88	-0.90	-0.07	-0.10
$\Delta Q(\text{MgO})$	0.43 (0.28)	0.43 (0.27)	0.02 (-0.08)	0.16 (0.06)
$\Delta Q(\text{Ag})$	0.45 (0.46)	0.47 (0.46)	0.05 (0.06)	-0.07 (-0.07)

<sup>a</sup> Values in parentheses are the population changes in interface MgO and Ag layers.

Geometric changes in the adsorbate and substrate, especially rumpling at the oxide–metal interface, have been reported to be important in explaining changes in the chemical reactivity of oxide films.<sup>8,9</sup> In the case of ultrathin MgO films with interface defects, the structures of both adsorbate and substrate are strongly affected by charge localization at the oxide–metal interface. For non-dissociative molecular adsorption (A) onto MgO/Ag(100) with  $\text{int-O}_{\text{vac}}$ , the  $\text{O}_{\text{w}}\text{-Mg1}$  and  $\text{H1-O}_{\text{s}}$  bond lengths decrease by 0.11 and 0.18 Å, respectively, compared to those of ND MgO film. Accordingly, the symmetric vibrational energy of the adsorbed water molecule decreases markedly by 76 meV due to the existence of  $\text{int-O}_{\text{vac}}$ . Thus, the weakened O–H bond of the adsorbed water molecule is more easily dissociated (see Table S2 for the detailed structure of the adsorbate). Layer rumpling during water dissociation is also severely affected by electron localization at the interface. Strong rumpling at the MgO/Ag(100) interface means that the adhesion between MgO and Ag layers becomes stronger with increasing covalent character.<sup>8</sup> The rumpling values (MgO:Ag, in Å) of the interface layers before dissociation of the water molecule (S) are 0.14:0.47, 0.44:0.20, and 0.32:0.46 for  $\text{int-O}_{\text{vac}}$ ,  $\text{int-Mg}_{\text{imp}}$ , and  $\text{int-O}_{\text{imp}}$ , respectively, while the ND MgO film shows negligible rumpling (see Table S3 and Figure S2 for details on layer rumpling). As a consequence, the adhesion energies between MgO film and Ag substrate with  $\text{int-O}_{\text{vac}}$ ,  $\text{int-Mg}_{\text{imp}}$ , and  $\text{int-O}_{\text{imp}}$  increase by 1.34, 0.60, and 0.71 eV, respectively, compared to that of ND MgO film. During water dissociation, the rumpling of interface layers increases in the order  $\text{int-O}_{\text{vac}} > \text{int-Mg}_{\text{imp}} \sim \text{int-O}_{\text{imp}}$ , which indicates that the rumpling of interface layers is closely correlated with the chemical reactivity of ultrathin MgO film.

Finally, we investigated the influence of interface defects on the adsorption properties of adsorbates with different electron affinities (EA) on ultrathin oxide films. Charging the adsorbate is considered significant for controlling such adsorption properties as structure and energy. This has been described by both work function ( $\Phi$ ) reduction and high EA of various adsorbates, such as  $\text{O}_2$ ,  $\text{N}_2\text{O}$ , and Au atoms or clusters.<sup>3–6,11,30</sup> The  $\Phi$  of 2-ML MgO/Ag(100) has been reported to be significantly reduced by  $1.4 \pm 0.2$  eV compared with that of free Ag(100) substrate using Kelvin probe force microscopy,<sup>31</sup> in good agreement with the computational data<sup>26b</sup> (1.2 eV). Therefore, it is important to evaluate how much  $\Phi$ , as one of the decisive parameters controlling adsorption, changes due to interface defects. The calculated work-function changes ( $\Delta\Phi$ ) with defect density<sup>20</sup> for MgO films with  $\text{int-O}_{\text{vac}}$ ,  $\text{int-Mg}_{\text{imp}}$ , and  $\text{int-O}_{\text{imp}}$  are -0.17, -0.12, and +0.19 eV, respectively, with respect to ND MgO/Ag(100).

This indicates that the charging effect of adsorbates on an oxide film surface can be further tailored by controlling the type and density of interface defects. However, we recently observed that the adsorption and dissociation of water molecules on MgO/Ag(100) cannot be explained by the charge-transfer mechanism alone, because the adsorbates produced during adsorption and dissociation have small EA values.<sup>8</sup> Therefore, in Table 2, we examine the influence of  $\text{int-O}_{\text{vac}}$  on the charging of  $\text{O}_2$  and  $\text{H}_2\text{O}$ , adsorbates with high and low EA, respectively (see Figure S3 for optimized structures of  $\text{O}_2/\text{MgO}/\text{Ag}(100)$  with and without  $\text{int-O}_{\text{vac}}$ ). MgO/Ag(100) has been suggested as a promising potential CO oxidation catalyst due to the charging of the reactant, i.e.  $\text{O}_2$ , via electron tunneling.<sup>6</sup> For both non-defective and defective ( $\text{int-O}_{\text{vac}}$ ) MgO/Ag(100), the  $\text{O}_2$  molecule is charged by about  $-0.9e$ , but the  $\text{H}_2\text{O}$  molecule is charged by just about  $-0.1e$ .<sup>32</sup> The charge gain of  $\text{O}_2$  molecule is mainly transferred from the interface layer.<sup>6</sup> While the amount of charge transfer from substrate to adsorbate does not depend on the existence of  $\text{int-O}_{\text{vac}}$ , the non-dissociative adsorption energy,  $E(A)$ , depends strongly on interface defects due to the above-mentioned change of charge distribution on the oxide surface. The  $E(A)$  of  $\text{O}_2$  and  $\text{H}_2\text{O}$  on the MgO film surface with  $\text{int-O}_{\text{vac}}$  are greater than those for the ND MgO film by 0.50 and 0.16 eV, respectively. This implies that the chemical reactions on the ultrathin oxide film surface can be controlled by defects located at the oxide–metal interface, regardless of whether the molecules are activated by charge transfer from the substrate. In addition, as mentioned above, the increase of charge gain due to  $\text{int-O}_{\text{vac}}$  is negligible for both  $\text{O}_2$  and  $\text{H}_2\text{O}$ , although the work function of the defective MgO film with  $\text{int-O}_{\text{vac}}$  is 0.17 eV smaller than that of the ND MgO film. This small change in charge transfer due to the interface defect would originate in the charging capacity of  $\text{O}_2$  and the small EA of  $\text{H}_2\text{O}$ . Therefore, in order to reveal in detail the relationship between the  $\Delta\Phi$  of the oxide film due to interface defects and the adsorption property, further study using additional kinds of adsorbates with various EA is required.

In summary, our computational results clearly show that the catalytic activity of ultrathin MgO films supported by Ag(100) substrate can be enhanced by introducing interface defects such as  $\text{int-O}_{\text{vac}}$ ,  $\text{int-Mg}_{\text{imp}}$ , and  $\text{int-O}_{\text{imp}}$ . This is closely correlated with the accompanying change of charge distribution of the oxide surface due to the strong localization of transferred charge density at the oxide–metal interface. In addition, the chemical reactions on the ultrathin oxide film surface can be tuned by interface defects regardless of the charging of adsorbates. A recent experimental study has reported that the dissociation probability of water on the monolayer MgO film surface is 6 times higher than that on bulk MgO.<sup>14,33</sup> Our result implies that buried interface defects would be one of the origins for the enhancement of chemical reactivity for water dissociation.

This study of interface defects not only reveals the potential of an ultrathin oxide film as a heterogeneous catalyst but also opens new vistas for the development of techniques for the control and measurement of the interface structure of oxide films deposited on a metal substrate. Control over interface defects might be obtained by systematic tuning of growth conditions or post-treatment of the oxide film.<sup>34</sup>

## ■ ASSOCIATED CONTENT

**S** Supporting Information. Computational details, reaction energies, ELF maps, selected geometric parameters of adsorbate,



layer rumpling values, and side views of the structure during water dissociation. This material is available free of charge via the Internet at <http://pubs.acs.org>.

## AUTHOR INFORMATION

### Corresponding Author

ykim@riken.jp; maki@k.u-tokyo.ac.jp

### Present Addresses

<sup>5</sup>School of Mechanical and Advanced Materials Engineering, Ulsan National Institute of Science and Technology, Ulsan 689-798, Republic of Korea

## ACKNOWLEDGMENT

This work was supported in part by a Grant-in-Aid for Scientific Research on Priority Areas “Electron Transport through a Linked Molecule in Nano-scale” and a Grant-in-Aid for Scientific Research(S) “Single Molecule Spectroscopy using Probe Microscope” from the Ministry of Education, Culture, Sports, Science, and Technology (MEXT), Japan, and in part by the Global COE Program (Chemistry Innovation through Cooperation of Science and Engineering), MEXT, Japan. We are grateful for the computational resources of the RIKEN Integrated Cluster of Clusters (RICC) supercomputer system. J.J. acknowledges the International Program Associate of RIKEN for support. We thank David W. Chapman for carefully reading the manuscript.

## REFERENCES

- (1) (a) Freund, H.-J. *Surf. Sci.* **2007**, *601*, 1438. (b) Freund, H.-J.; Pacchioni, G. *Chem. Soc. Rev.* **2008**, *37*, 2224. (c) Risse, T.; Shaikhutdinov, S.; Nilius, N.; Sterrer, M.; Freund, H.-J. *Acc. Chem. Res.* **2008**, *41*, 949. (d) Nilius, N. *Surf. Sci. Rep.* **2009**, *64*, 595. (e) Harding, C.; Habibpour, V.; Kunz, S.; Farnbacher, A. N.-S.; Heiz, U.; Yoon, B.; Landman, U. *J. Am. Chem. Soc.* **2009**, *131*, 538. (f) Ulrich, S.; Nilius, N.; Freund, H.-J.; Martinez, U.; Giordano, L.; Pacchioni, G. *Phys. Rev. Lett.* **2009**, *102*, 016102. (g) Freund, H.-J. *Chem. Eur. J.* **2010**, *16*, 9384. (h) Farmer, J. A.; Campbell, C. T. *Science* **2010**, *329*, 933.
- (2) Sterrer, M.; Yulikov, M.; Risse, T.; Freund, H.-J.; Carrasco, J.; Illas, F.; Di Valentin, C.; Giordano, L.; Pacchioni, G. *Angew. Chem. Int. Ed.* **2006**, *45*, 2633.
- (3) Hellman, A.; Grönbeck, H. *Phys. Rev. Lett.* **2008**, *100*, 116801.
- (4) Grönbeck, H. *J. Phys. Chem. B* **2006**, *110*, 11977.
- (5) Starr, D. E.; Weis, C.; Yamamoto, S.; Nilsson, A.; Bluhm, H. *J. Phys. Chem. C* **2009**, *113*, 7355.
- (6) Hellman, A.; Klacar, S.; Grönbeck, H. *J. Am. Chem. Soc.* **2009**, *131*, 16636.
- (7) Honkala, K.; Hellman, A.; Grönbeck, H. *J. Phys. Chem. C* **2010**, *114*, 7070.
- (8) Jung, J.; Shin, H.-J.; Kim, Y.; Kawai, M. *Phys. Rev. B* **2010**, *82*, 085413.
- (9) Carrasco, E.; Brown, M. A.; Sterrer, M.; Freund, H.-J.; Kwapien, K.; Sierka, M.; Sauer, J. *J. Phys. Chem. C* **2010**, *114*, 18207.
- (10) Schintke, S.; Messerli, S.; Pivetta, M.; Patthey, F.; Lioubille, L.; Stengel, M.; De Vita, A.; Schneider, W.-D. *Phys. Rev. Lett.* **2001**, *87*, 276801.
- (11) Ricci, D.; Bongiorno, A.; Pacchioni, G.; Landman, U. *Phys. Rev. Lett.* **2006**, *97*, 036106.
- (12) Honkala, K.; Häkkinen, H. *J. Phys. Chem. C* **2007**, *111*, 4319.
- (13) Shin, H.-J.; Jung, J.; Motobayashi, K.; Yanagisawa, S.; Morikawa, Y.; Kim, Y.; Kawai, M. *Nat. Mater.* **2010**, *9*, 442.
- (14) (a) Savio, L.; Celasco, E.; Vattuone, L.; Rocca, M. *J. Chem. Phys.* **2003**, *119*, 12053. (b) Savio, L.; Celasco, E.; Vattuone, L.; Rocca, M. *J. Phys. Chem. B* **2004**, *108*, 7771.
- (15) Altieri, S.; Contri, S. F.; Valeri, S. *Phys. Rev. B* **2007**, *76*, 205413.
- (16) (a) Reissner, R.; Radke, U.; Schulze, M.; Umbach, E. *Surf. Sci.* **1998**, *402–404*, 71. (b) Schulze, M.; Reissner, R. *Surf. Sci.* **2001**, *482–485*, 285.
- (17) Ozensoy, E.; Peden, C. H. F.; Szanyi, J. *J. Phys. Chem. B* **2005**, *109*, 15977.
- (18) (a) Sun, Y.-N.; Qin, Z.-H.; Lewandowski, M.; Carrasco, E.; Sterrer, M.; Shaikhutdinov, S.; Freund, H.-J. *J. Catal.* **2009**, *266*, 359. (b) Sun, Y.-N.; Giordano, L.; Goniakowski, J.; Lewandowski, M.; Qin, Z.-H.; Noguera, C.; Shaikhutdinov, S.; Pacchioni, G.; Freund, H.-J. *Angew. Chem. Int. Ed.* **2010**, *49*, 4418.
- (19) (a) Lambert, C.; Groppo, E.; Prestipino, C.; Casassa, S.; Ferrari, A. M.; Pisani, C.; Giovanardi, C.; Luches, P.; Valeri, S.; Boscherini, F. *Phys. Rev. Lett.* **2003**, *91*, 046101. (b) Maurice, V.; Despert, G.; Zanna, S.; Bacos, M.-P.; Marcus, P. *Nat. Mater.* **2004**, *3*, 687.
- (20) Spin-polarized periodic DFT calculations were performed with the projector-augmented wave method and the Perdew–Wang exchange–correlation functional (PW91) at the single molecule level.  $(2\sqrt{2}\times 2\sqrt{2})R45^\circ$  surface supercells are used to remove the intermolecular interaction among neighboring adsorbates on the surfaces. See Supporting Information for details.
- (21) An impurity oxygen atom in the interface Ag layer locates at the hollow site instead of at the atomic position of Ag due to strong ionic interaction with  $Mg^{2+}$  of the interface MgO layer. This repositioning of the oxygen atom stabilizes the system by 1.2 eV.
- (22) (a) Lopez, N.; Valeri, S. *Phys. Rev. B* **2004**, *70*, 125428. (b) Carrasco, J.; Lopez, N.; Illas, F.; Freund, H.-J. *J. Chem. Phys.* **2006**, *125*, 074711.
- (23) The formation energies of O vacancies were calculated taking the reference energy for an O atom to be half the total energy of an O<sub>2</sub> molecule in the gas phase.
- (24) Yuasa, S.; Nagahama, T.; Fukushima, A.; Suzuki, Y.; Ando, K. *Nat. Mater.* **2004**, *3*, 868.
- (25) Carrasco, J.; Illas, F.; Lopez, N. *Phys. Rev. Lett.* **2008**, *100*, 016101.
- (26) (a) Goniakowski, J.; Noguera, C. *Interface Sci.* **2004**, *12*, 93. (b) Giordano, L.; Cinquini, F.; Pacchioni, G. *Phys. Rev. B* **2005**, *73*, 045414.
- (27) (a) Henkelman, G.; Arnaldsson, A.; Jónsson, H. *Comput. Mater. Sci.* **2006**, *36*, 354. (b) Tang, W.; Sanville, E.; Henkelman, G. *J. Phys.: Condens. Matter* **2009**, *21*, 084204.
- (28) All Bader charges presented here were calculated in a  $(2\sqrt{2}\times 2\sqrt{2})R45^\circ$  supercell composed of four Ag layers and two MgO layers.
- (29) (a) Yoon, B.; Häkkinen, H.; Landman, U.; Wörz, A. S.; Antonietti, J.-M.; Abbet, S.; Judai, K.; Heiz, U. *Science* **2005**, *307*, 403. (b) Yan, Z.; Chinta, S.; Mohamed, A. A.; Fackler, J. P., Jr.; Goodman, D. W. *J. Am. Chem. Soc.* **2005**, *127*, 1604.
- (30) (a) Pacchioni, G.; Giordano, L.; Baistrocchi, M. *Phys. Rev. Lett.* **2005**, *94*, 226104. (b) Sterrer, M.; Risse, T.; Pozzoni, U. M.; Giordano, L.; Heyde, M.; Rust, H.-P.; Pacchioni, G.; Freund, H.-J. *Phys. Rev. Lett.* **2007**, *98*, 096107. (c) Simic-Milosevic, V.; Heyde, M.; Nilius, N.; König, T.; Rust, H.-P.; Sterrer, M.; Risse, T.; Freund, H.-J.; Giordano, L.; Pacchioni, G. *J. Am. Chem. Soc.* **2008**, *130*, 7814.
- (31) Bielezki, M.; Hynninen, T.; Soini, T. M.; Pivetta, M.; Henry, C. R.; Foster, A. S.; Esch, F.; Barth, C.; Heiz, U. *Phys. Chem. Chem. Phys.* **2010**, *12*, 3203.
- (32) Formation of O<sub>2</sub><sup>•-</sup> radical anion on MgO film grown on Mo(100) substrate was recently confirmed by EPR spectroscopy: Gonchar, A.; Risse, T.; Freund, H.-J.; Giordano, L.; Di Valentin, C.; Pacchioni, G. *Angew. Chem. Int. Ed.* **2011**, *50*, 2635.
- (33) Experimental observation reveals that Ag bare surface and multilayer MgO islands still coexist with 1-ML island.
- (34) Defect control at the interface with various film growth conditions has been of great importance in research on complex oxide materials: (a) Herranz, G.; Basletić, M.; Bibes, M.; Carrétero, C.; Tafra, E.; Jacquet, E.; Bouzouane, K.; Deranlot, C.; Hamzić, A.; Broto, J.-M.; Barthélémy, A.; Fert, A. *Phys. Rev. Lett.* **2007**, *98*, 216803. (b) Siemons, W.; Koster, G.; Yamamoto, H.; Geballe, T. H.; Blank, D. H. A.; Beasley, M. R. *Phys. Rev. B* **2007**, *76*, 155111.